Structure and Phase Equilibria of Polyelectrolytic Hairy-Rod Supramolecules in the Melt State

Matti Knaapila,*,‡ Roman Stepanyan,§,# Lockhart E. Horsburgh,||,⊥ Andrew P. Monkman,|| Ritva Serimaa,‡ Olli Ikkala,† Andrei Subbotin,§ Mika Torkkeli,‡ and Gerrit ten Brinke†,§

Division of X-ray Physics, Department of Physical Sciences, P.O. Box 64, University of Helsinki, FIN-00014 Finland, Department of Polymer Science and Material Science Center, University of Groningen, Nijenborgh 4, 9747 AG Groningen, The Netherlands, Department of Physics, University of Durham, South Road, Durham, DH1 3LE, United Kingdom, and Department of Engineering Physics and Mathematics, Helsinki University of Technology, P.O. Box 2200, FIN-02015 HUT, Finland

Received: June 25, 2003; In Final Form: September 29, 2003

The structure formation and phase behavior of supramolecular hairy-rod polymers consisting of rodlike polymer chains with physically bonded side chains are investigated in the melt state using small-angle X-ray scattering. The supramolecules consist of poly(2,5-pyridinediyl), complexed by methanesulfonic acid to form poly(2,5-pyridinium methane sulfonates), to which octyl gallates are hydrogen bonded. These comblike supramolecules self-organize in rodlike assemblies in a square or oblique lattice or form lamellar structures. Moreover, nematic (solid) and macrophase separated structures are observed. These results are collected in a phase diagram in the high polymer fraction limit and they are in a clear qualitative resemblance with recent theoretical modeling. The differences and similarities between the experiments and theory are discussed.

1. Introduction

Hairy-rod polymers consist of a rigid or semirigid backbone where a dense set of side chains is bonded in a comb-shaped manner.[1−7] The concept allows self-organization and improved solubility even for polymers of rigid rodlike backbone. Unlike hairy-rod polymers with rodlike polymer backbone and covalently bonded flexible side chains, supramolecular hairy-rod polymers have the side groups connected to the backbone by physical bonds,[8−14] see Scheme 1. Theoretical treatments of the self-organized structure formation of hairy-rod polymers[15] and supramolecular hairy-rod polymers[16] have recently been presented. These theories predict that hexagonal, oblique, and lamellar microphase separated structures as well as isotropic phase are typically present for hairy rods, see Scheme 1.

Understanding the phase behavior of hairy rods[15] is important to design liquid crystallinity[17,18] which allows facile alignment of the otherwise crystalline infusible and intractable polymers. With conjugated polymers,[19,20] the alignment results in anisotropy of their optical[12,13] and electronic[21] properties. The alignment of conjugated hairy rods in thin films can also result in completely new structural features[22] compared to the bulk. When specific side chains are employed, the resultant rich photonic phenomena, such as circularly polarized luminescence,[23] give another reason for their study. In contrast to the covalently bonded ones, the coils and rods of the supramolecular hairy rods characteristically tend to macroscopically phase separate, because of small mixing entropy and aggregation tendency of the rods, thus requiring a particularly strong attractive interaction between the rods and coils. The side chains can also be removed after alignment, thus yielding aligned pristine material.[12,13] The direct comparison of the melt-state phase behavior of supramolecular hairy rods between the experiment and theory seems to be scarce. We have carried out experiments to investigate the structure and phase behavior of supramolecular hairy rods. Experimentally, there is considerable

SCHEME 1. (a) A Model of a Thermoreversible Hairy-Rod Molecule[a] (b) Chemical Formula of $PPY(MSA)_{1.0}(OG)_{1.0}$ (c) The Proposed Observed Microstructures Viewed along the Polymer Microdomains[b]

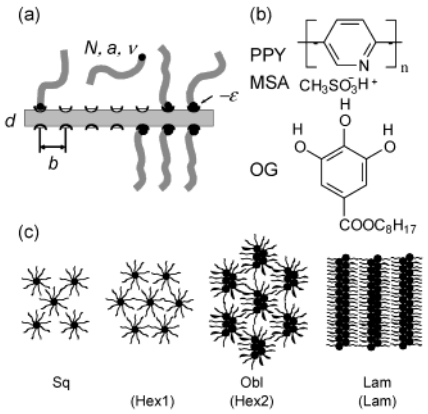

[a] *N*, *a*, and ν are the number of segments, the segment length, and the volume; *b* is the distance between active sites on a rigid rod, and *d* is the rod diameter. [b]Square, Sq; elliptical oblique, obl; and lamellar, Lam, structure. The notations used in theory are in parentheses. In theory a true hexagonal phase (Hex1) is additionally predicted.

* Corresponding author. Present address: Department of Physics, University of Durham, South Road, Durham DH1 3LE, United Kingdom; tel: +44-191-334-3520; fax: +44-191-334-3585; email: matti.knaapila@durham.ac.uk.

‡ University of Helsinki.

§ University of Groningen.

|| University of Durham.

† Helsinki University of Technology.

⊥ Present address: Avocado Research Chemicals, Shore Road, Heysham, Lancashire, LA3 2XY, United Kingdom.

Present address: Physics of Complex Fluids, Department of Applied Physics, University of Twente, P.O. Box 217, 7500 AE Enschede, The Netherlands.

10.1021/jp035810m CCC: $25.00
Published on Web 12/02/2003

complexity in the specifics of the structures and structural phase behavior but, overall, one can identify general features that are in agreement with recent theoretical treatments.[16] Furthermore, the theory gives us a hint (at least qualitatively) in which direction the experimental system has to be adjusted to get desired effects.

2. Theoretical Background

In the hairy-rod supramolecules of interest, the backbone and side chains are both chemically and geometrically different—being rodlike and flexible—and they tend to microphase separate, that is, self-organize, to form rod-rich and coil-rich microdomains. The interaction between the moieties is generally described using the Flory−Huggins χ−parameter, but in the strong segregation limit considered here a more convenient parameter is the surface tension γ which is proportional to $\chi\delta$, where δ is the width of the interpenetration region between the pure rod and pure coil phase. Experimentally, the existence of sharp interfaces in the class of materials studied here has been demonstrated recently.[14] Within the strong segregation approach, the occurrence of various self-organized morphologies (cf. Scheme 1) depends on the balance between two competing contributions to the free energy. These are on one hand the unfavorable contacts between the rods and coils depending on the interface area S and on the other hand the stretching of the flexible side chains because of the microphase separation. The total free energy F takes the form[15]

$$\frac{F}{T} \cong \frac{\gamma}{T}S + \frac{F_{el}}{T} \qquad (1)$$

Because the stretching energy F_{el} is purely entropic (proportional to the temperature T), for low temperatures the first term dominates, while at higher temperature the elastic part becomes more important. S and F_{el} for different structures may be calculated from the knowledge of a certain set of parameters: N, the number of monomers in the coil, and $\kappa = \nu/(\pi d^2 b/4)$ the ratio between the volumes of a coil monomer and the backbone section between two consecutive branching sites. Here, the parameters d and b describe the size of the backbone, see Scheme 1. In the covalent hairy rods, minimization of the free energy as a function of the volume fraction of rods f for various microphase-separated morphologies predicts[15] the lamellar (Lam) and two types of cylindrical morphologies, denoted by Hex1 and Hex2, as depicted in Scheme 1. Spherical structures do not occur. In addition, a nematic (solid) (Nem) structure is expected for very short side chains, and at very high temperatures the system becomes disordered (isotropic) when the side chains are long enough.

In the supramolecular case, which is of interest here, macrophase separation into nematic rod-rich and isotropic coil-rich phases also becomes possible. In fact, because of the limited mixing entropy of rodlike polymers,[24] simple rod−coil mixtures tend to macrophase separate into almost pure components and microphase separation occurs only in the case of strong association. The possibility of macrophase separation distinguishes the theoretical consideration of supramolecular hairy rods from that of the covalent hairy rods and also limits the number of suitable materials to test the model in practice. The most fundamental consequence is that now the volume fraction of rods f within the microphase-separated phase is a free parameter. It depends on the energy of association, $-\epsilon$, from which the grafting density may differ from the amount of coils that is originally put in the sample. Besides this fact, the consideration is the same as for covalent hairy rods including a comparison of free energies of the possible phases to find phase boundaries as a function of T and f for a given $-\epsilon$. The outcome of the theory is different depending on the effect of the stretching energy. When the side chains are long enough for the stretching energy to be important, three different types of phase diagrams have been predicted.[16] For small ϵ only nematic, isotropic, and lamellar phases occur. For increased ϵ, we also obtain the other microstructured phases, first only Hex2 and finally for large ϵ we obtain all the microphases introduced above, thus approaching the covalently bonded case. When the side chains are short enough, the stretching energy may be omitted from the theory. As a result, the lamellar microphase now occupies a large part of the phase diagram and no other microstructured phases are predicted. This result is presented in Figure 1.

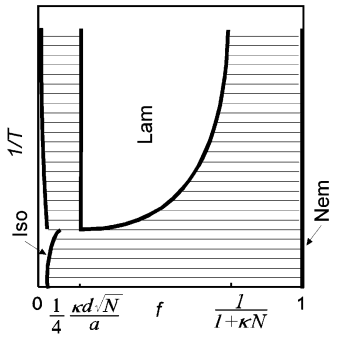

Figure 1. Theoretical phase diagram, corresponding to the $\kappa N < 1$ case, with f the rod volume and $1/T$ the inverse temperature.

3. Experimental Section

Rodlike poly(2,5-pyridinediyl) (PPY) was first complexed with a stoichiometric amount of methanesulfonic acid (MSA) which forms a poly(2,5-pyridinium methane sulfonate) denoted $PPY(MSA)_{1.0}$. It was further complexed with a 1-octyl-3,4,5-trihydroxybenzoate, that is, octyl gallate (OG) to form a complex denoted henceforth $PPY(MSA)_{1.0}(OG)_y$ where y equals the molar ratio between OG and PPY monomers, see Scheme 1. PPY is of a very high quality and its synthesis and characterization have been reported in detail.[25−27] PPY is not a mixture of isomers but there is an issue of regioregularity within the polymer which is a mixture of head-to-head and head-to-tail linkages. This does not significantly affect the rigid-rod properties. All the complexes were made in dilute solutions of formic acid followed by evaporation and drying in a vacuum. The complexes were studied using small-angle X-ray scattering (SAXS). Macrophase separation and birefringence were studied using optical microscopy with crossed polarizers, and differential scanning calorimetry (DSC) was used to study the thermal transitions. The detailed preparation of complexes and the employed methods have been described elsewhere.[8,14]

4. Results and Discussion

In this study, the conjugated rodlike polymer poly(2,5-pyridinediyl), PPY, was used. There are several approaches to form supramolecular hairy-rodlike structures on the basis of PPY type materials.[28,29] The method of combining protonation and hydrogen bonding has been used for polyaniline based materials.[30] It is also feasible for simultaneous control of structural and optoelectronic properties of PPY-based materials.[31,32] Therefore, the combination of protonation and hydrogen bonding was used here as well. MSA protonates PPY and the complex

$PPY(MSA)_{1.0}$ contains sulfonates as hydrogen-bonding acceptors which allow hydrogen bonding with OG to yield $PPY(MSA)_{1.0}(OG)_y$. Therefore, the actual material is a more complicated analogue to the model compounds referenced in the theoretical analysis of ref 16. The backbones are charged polyelectrolytes and the flexible coils are short and have several hydrogen-bonding donors which help suppress the macrophase separation, see Scheme 1a. In the theoretical model, it turns out that the hairy rods in the microphases have the majority of their active sites occupied by the associated coils. In the experiment, as we will see, such a condition may not be totally achieved. Also, OG contains a large polar headgroup with three associating sites and only the alkyl chain is regarded as a flexible side chain. Thus, the experimental rod consists of PPY, MSA, and the polar part, head of OG. Moreover, the theory deals with completely rodlike polymers, whereas the persistence length of this class of polymers is obviously finite, for example, 75−200 Å for alkyl substituted poly(*p*-phenylenes).[33]

Experimentally, we find microphase-separated uniform phases when $y < 2.0$, and therefore the amount of side chains was chosen around this value ($y = 0.2$, 0.5, 0.75, 1.0, 1.5, 2.0, 2.5, and 3.0). The rod concentration, $f \cong (1 + 0.9y)/(1 + 1.6y)$, in this work was relatively high. It was selected as such not only for the purpose of avoiding possible macrophase separation but also because the most interesting photonic phenomena generally appear for low y. Therefore, κN is below unity and the side chains are so short that their stretching seems relatively unimportant; hence, the bond energy $-\epsilon$ becomes the determining factor for the phase diagram.[16]

Several predictions made on the basis of the theoretical consideration may be verified. PPY and $PPY(MSA)_{1.0}$ are infusible and crystalline at least between 25 and 220 °C, above which $PPY(MSA)_{1.0}$ decomposes. PPY is stable at these temperatures.[34] A strong tendency to self-organization, which has the same generic features as in the covalent hairy-rod system,[15] arising from the mutual repulsion between rods and coils[16] is found already when a very small amount of OG is added. The corresponding SAXS peak is seen at $q \approx 0.2$ Å^{-1} for $y \geq 0.2$. Like crystalline PPY, the self-organized material is yellow and highly birefringent. The self-organization is directly related to the existence of a melt state, which also connects the observations to the theory where the melt state is assumed a priori.[16] For small y, the structure is still relatively poor. When the amount of side chains is increased to $y = 0.50-0.75$, the reflection becomes sharper and higher order peaks are seen at $\sqrt{n}q^*$, where $n = 1, 2, 4, 5,...$. The structure is identified as the square (Sq) phase. Increasing y further, at $y = 1.0$, the lattice changes into oblique. It is denoted as Obl and tentatively corresponds to the theoretically predicted Hex2 phase, see Scheme 1. Figure 2 shows the SAXS pattern of $PPY(MSA)_{1.0}(OG)_{1.0}$ in the melt state at 110 °C clearly demonstrating this situation. The positions of the reflections follow the suggestive indexation on the basis of oblique lattice. Though there are several components present, neither PPY nor $PPY(MSA)_{1.0}$ show reflections at the low scattering angles and pure MSA is a liquid. Further, the diffraction measurements were made above the melting point of OG ($T_m \sim 102$ °C) to make sure that possible crystalline OG does not contribute to the SAXS patterns.

The lamellar phase is present for $y > 1.5$, while for $y > 2.0$ macrophase separation starts gradually to occur. The case $y = 2.0$ has been previously found to form a lamellar phase.[10] If PPY organizes in π-stacks as is assumed (see below), the observed lamellar period 29.7 Å, the repeat length 4.3 Å, and the stack distance ca. 3.5 Å would indicate that only 80% of the bonding sites are occupied. Therefore, a minor macrophase-separated phase is expected to coexist, even though the material looks uniform at optical resolution. For small and high y values, that is, $y = 0.2$ and $y = 3.0$, the microphase-separated structures are not very well defined but the long periods do not differ from the structures at the nearest phase domains and therefore their morphologies are suggested to correspond to them.

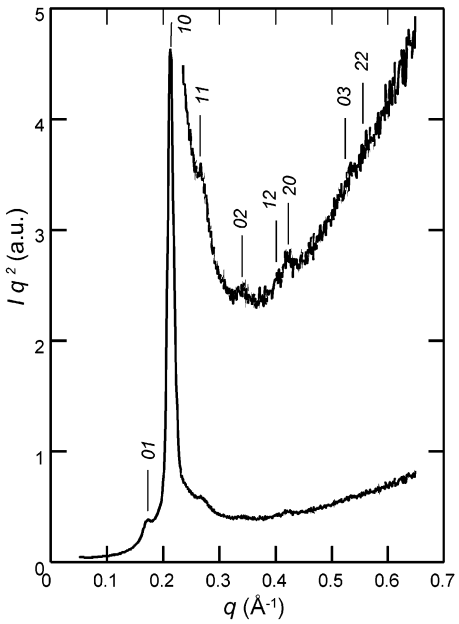

Figure 2. X-ray diffraction pattern of $PPY(MSA)_{1.0}(OG)_{1.0}$ in the melt state at 110 °C suggesting the existence of oblique phase (Obl). Clear peaks are observed at 0.171 Å^{-1}, 0.214 Å^{-1}, 0.271 Å^{-1}, 0.341 Å^{-1}, and 0.42 Å^{-1}.

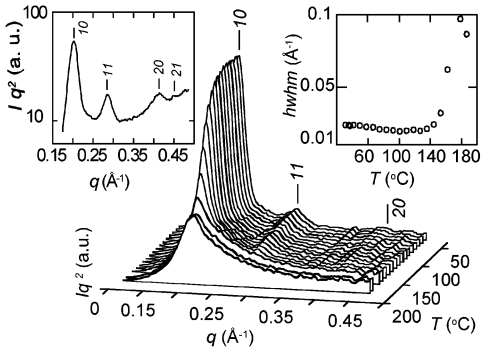

Figure 3. The SAXS patterns during slow cooling of $PPY(MSA)_{1.0}(OG)_{0.75}$ showing order−disorder transition (ODT) at ca. $T_{ODT} = 140$ °C. The inserts show the details of the diffraction pattern below ODT and the HWHM of the reflection *10*.

The above compositions were also thoroughly studied in the temperature range 25−220 °C and the melt state is obtained above $T > 110$ °C. The material decomposes at $T > 220$ °C if left there for a long time. However, in a sealed sample holder and under nitrogen atmosphere the material could hold out for tens of minutes at 190 °C. During heating, there is, except at very small y, an order−disorder transition (ODT) from a microphase-separated phase to an isotropic phase or to coexistent isotropic and nematic phases as revealed by the sudden decrease in the width of the *10* reflection, see Figure 3. For the square phase (Sq), $T_{ODT} = 140$ °C, but for Obl and Lam this increases to $T_{ODT} = 180$ °C. This contradicts theory, where Hex2 is predicted to be stable at higher temperatures. The ODT is also verified using differential scanning calorimetry (DSC), showing

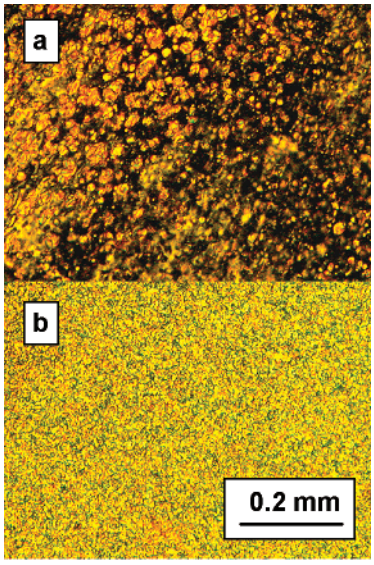

Figure 4. The optical micrographs with crossed polarizers of PPY-$(MSA)_{1.0}(OG)_{0.75}$ corresponding to the situation in Figure 3 show the coexistence of isotropic phase and suggested liquid crystalline droplets $T = 160$ °C, above ODT, (a). Uniformly birefringent phase at $T = 130$ °C, below ODT, (b). Both are fluid substances. Adapted from ref 8.

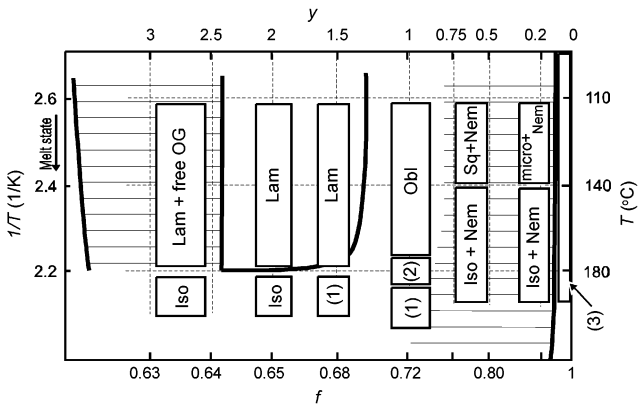

Figure 5. Experimental compilation of the observations on PPY-$(MSA)_{1.0}(OG)_y$. Here, f is the rod volume assuming a single microphase and $1/T$ is the inverse temperature. The vertically drawn labels are based on SAXS and optical microscopy; (1) corresponds to almost pure Iso phase, (2) to the coexistence between Obl and Iso, and (3) is crystalline material which starts to be plastiziced and microphase separated. The binodal lines are drawn to guide the eye. The crossed areas are regions of coexistence.

a distinct peak at the same temperature with an abrupt increase of the half-width half-maximum of SAXS intensity.[8] Moreover, the phase transitions may be observed in optical microscopy with crossed polarizers (cf. Figure 4) and as expected the isotropic phase shows no birefringence. Above the ODT, rods and coils tend to separate into nematic and isotropic phases in the molten state for $y < 1.5-2.0$. The nematic phase is not pure $PPY(MSA)_{1.0}$, since this is crystalline at the studied temperatures, but contains a small fraction of penetrated coils. Only the melt state shows ionic conductivity, and there is a small change in conductivity at the ODT.[8] However, when the microphase-separated phase is present, the presence of the nematic phase is hard to establish, since the samples are uniformly yellow and birefringent.

The observations are gathered in a temperature−concentration diagram presented in Figure 5. The pertinent theoretically predicted phase diagram is shown in Figure 1. The binodal lines drawn on the basis of experiments are relatively consistent with the theory where the lamellar domain dominates. The systems studied always had a significant rod volume fraction in which case the theory predicts only a large region of stability for the Lam phase. Several aspects of the phase behavior predicted by the theory are indeed observed. When ϵ is small or T high, the association is not able to compete with the strong tendency for macrophase separation and the system segregates into almost pure rod- and coil-rich phases.[24] For somewhat higher values of ϵ, a region occurs where coils and rods become partially compatible and capable of forming hairy-rod supramolecules. This region is also susceptible to microstructure formation.

A striking difference between experiment and theory concerns the existence of the Obl (Hex2) phase, which theoretically only occurs for $\kappa N > 1$. Moreover, the single hexagonal phase Hex1, that is theoretically predicted, is not observed at all. Instead the square phase, Sq, is found. Theoretically, the square phase was always suppressed by Hex1, albeit that the theory considered hairy rods of a single polymer. In the present case we may estimate, using a density of 1.5 g/cm^3, that the rods actually contain 10−12 polymer chains in parallel. Here, we assume one rod per unit cell, which is a fair assumption given that the unit cell dimension (ca. 30 Å) is comparable to twice the length of the side groups. It is not obvious what accounts for the differences between theory and experiment but we might guess that $\pi-\pi$ interaction plays an important part in this. Experiments show that conjugated PPY in this case as well as in previous work[12−14] tend to organize in stacks of ca. 3.5 Å periodicity. This is seen as a single scattering peak at wide angles (roughly $q = 1.8$ 1/Å) and is observed for all the microphase-separated cases studied here (data not presented). The observed behavior is even more appreciable than in thiophenes (e.g., polyoctylthiophenes), which are considered prime examples of such directed self-assembly by π-stacking.[35] This particularly manifests itself in the organization at surfaces and interfaces.[35,36,12,13] Here, the effect is likely enhanced by the aromatic headgroup in the amphihile. Thus, the current system might be likened to "*hairy boards*"[35] rather than rods.

In Obl, the unit cell dimensions are approximately $a \approx 29$ Å and $b \approx 37$ Å and by density arguments it contains ca. nine parallel polymer chains. The shape of the self-organized domains is likely to be elongated or elliptical. The *01* reflection is significantly lower than *10*, which might indicate almost parallel alignment of the microdomains in a lamellar-like fashion. This view is corroborated by the fact that b roughly corresponds to ca. 10 π-stacked polymer layers. In the lamellar phase, the lamellar period is the same as the lattice constant a in the Obl phase.

Other examples, including still shorter side chains, have been very extensively explored as well.[14] In the case where PPY is complexed with bulky camphorsulfonic acid and very short 5-pentyl-1,3-dihydroxybenzene or 4-hexyl-1,3-dihydroxybenzene, octyl phenol, or octyl gallate, besides the Iso and Nem phases only the lamellar structure is seen,[14] in strong support of the theoretical predictions.

5. Conclusions

The predictions of a recent theory for the structure and phase behavior of supramolecular hairy rods in the melt state have been compared with experimental results obtained using the $PPY(MSA)_{1.0}(OG)_y$ complexes. The theoretical picture can be summarized as follows. The associating rod-coil system may self-organize in three possible microstructures and form isotropic or nematic (solid) phases. The equilibrium is controlled by temperature, the association energy ϵ, and the length and grafting

density of the associated coils. Different regimes can be distinguished depending on ϵ and the rod volume. The theory partly agrees with the experimental observations, but clear differences are found as well. This might well be due to the experimental complex being much more complicated than the model assumes, primarily because of the large headgroups of the OG side chains. Differences may also arise from the presence of charged molecules.

In accordance with the theory, there is a strong tendency to microphase separation. There are three kinds of microphase-separated phases observed, two of which contain rodlike assemblies in square (Sq) and oblique (Obl) lattices, and the third phase is lamellar (Lam). The simple hexagonal phase (Hex1) was not observed. This is believed to reflect the tendency toward $\pi-\pi$-stacking which suppresses the existence of single hairy rods. The lamellar phase region indeed dominates the phase diagram, which agrees well with the theory, and rodlike morphologies occupy the high rod concentration end of the phase diagram. Contrary to the theory, the T_{ODT} is highest for the lamellar phase. The microphase-separated phases were observed to coexist only with Nem or Iso phases, but not together. Order−order phase transitions were not observed in the melt state. The isotropic phase is the single phase at low rod concentrations above ODT. At higher rod concentration, the isotropic phase coexists with birefringent droplets, regarded as a nematic phase.

Acknowledgment. The authors acknowledge Academy of Finland, National Technology Agency (Finland), The Netherlands Organization for Scientific Research (NWO), EPSRC, and Leverhulme Trust for grants.

References and Notes

(1) Ballauf, M. *Makromol. Chem., Rapid Commun.* **1986**, *7*, 407−414.
(2) Ballauf, M.; Schmidt, G. F. *Makromol. Chem., Rapid Commun.* **1987**, *8*, 93−97.
(3) Duran, R.; Ballauf, M.; Wenzel, M.; Wegner, G. *Macromolecules* **1988**, *21*, 2897−2899.
(4) Ballauf, M. *Angew. Chem., Int. Ed. Engl.* **1989**, *101*, 261−276.
(5) Watanabe, J.; Harkness, B. R.; Sone, M.; Ichimura, H. *Macromolecules* **1994**, *27*, 507−512.
(6) Lauter, U.; Meyer, W. H.; Wegner, G. *Macromolecules* **1997**, *30*, 2092−2101.
(7) Wegner, G. *Macromol. Chem. Phys.* **2003**, *204*, 347−357.
(8) Knaapila, M. Self-Organized Supramolecular Electroactive Polymers. Master's Thesis, Helsinki University of Technology, 1999.
(9) Ikkala, O.; Knaapila, M.; Ruokolainen, J.; Torkkeli, M.; Serimaa, R.; Jokela, K.; Horsburgh, L.; Monkman, A.; ten Brinke, G. *Adv. Mater.* **1999**, *11*, 1206−1210.
(10) Knaapila, M.; Ruokolainen, J.; Torkkeli, M.; Serimaa, R.; Horsburgh, L.; Monkman, A. P.; Bras, W.; ten Brinke, G.; Ikkala, O. *Synth. Met.* **2001**, *121*, 1257−1258.
(11) Knaapila, M.; Torkkeli, M.; Mäkelä, T.; Horsburgh, L.; Lindfors, K.; Serimaa, R.; Kaivola, M.; Monkman, A. P.; ten Brinke, G.; Ikkala, O. *Mater. Res. Soc. Symp. Proc.* **2001**, *660*, JJ5.21.1−6.
(12) Knaapila, M.; Ikkala, O.; Torkkeli, M.; Jokela, K.; Serimaa, R.; Dolbnya, I. P.; Bras, W.; ten Brinke, G.; Horsburgh, L. E.; Pålsson, L.-O.; Monkman, A. P. *Appl. Phys. Lett.* **2002**, *81*, 1489−1491.
(13) Knaapila, M.; Torkkeli, M.; Pålsson, L.-O.; Horsburgh, L. E.; Jokela, K.; Dolbnya, I. P.; Bras, W.; Serimaa, R.; ten Brinke, G.; Monkman, A. P.; Ikkala, O. *Mater. Res. Soc. Symp. Proc.* **2002**, *725*, 237−242.
(14) Knaapila, M.; Torkkeli, M.; Jokela, K.; Kisko, K.; Horsburgh, L. E.; Pålsson, L.-O.; Seeck, O. H.; Dolbnya, I. P.; Bras, W.; ten Brinke, G.; Monkman, A. P.; Ikkala, O.; Serimaa, R. *J. Appl. Crystallogr.* **2003**, *36*, 702−707.
(15) Stepanyan, R.; Subbotin, A.; Knaapila, M.; Ikkala, O.; ten Brinke, G. *Macromolecules* **2003**, *36*, 3758−3763.
(16) Subbotin, A.; Stepanyan, R.; Knaapila, M.; Ikkala, O.; ten Brinke, G., in preparation.
(17) Tashiro, K.; Ono, K.; Minagawa, Y.; Kobayashi, M.; Kawai, T.; Yoshino, K. *J. Polym. Sci., Part B: Polym. Phys.* **1991**, *29*, 1223−1233.
(18) Prosa, T. J.; Moulton, J.; Heeger, A. J.; Winokur, M. J. *Macromolecules* **1999**, *32*, 4000−4009.
(19) Winokur, M. J. Structural Studies of Conducting Polymers. In *Handbook of Conducting Polymers*; Skotheim, T. A., Elsenbaumer, R. L., Reynolds, J. R., Eds.; Marcel Dekker: New York, 1998; pp 707−726.
(20) Winokur, M. J.; Chunwachirasiri, W. *J. Polym. Sci., Part B: Polym. Phys.* **2003**, *41*, 2630−2648.
(21) Sirringhaus, H.; Wilson, R. J.; Friend, R. H.; Inbasekaran, M.; Wu, W.; Woo, E. P.; Grell, M.; Bradley, D. D. C. *Appl. Phys. Lett.* **2000**, *77*, 406−408.
(22) Knaapila, M.; Lyons, B. P.; Kisko, K.; Foreman, J. P.; Vainio, U.; Mihaylova, M.; Seeck, O. H.; Pålsson, L.-O.; Serimaa, R.; Torkkeli, M.; Monkman, A. P. *J. Phys. Chem. B* **2003**, *107*, 12425−12430.
(23) Langeveld-Voss, B. M. W.; Janssen, R. A. J.; Christiaans, M. P. T.; Meskers, S. C. J.; Dekkers, H. P. J. M.; Meijer, E. W. *J. Am. Chem. Soc.* **1996**, *118*, 4908−4909.
(24) Flory, P. J. *Adv. Polym. Sci.* **1984**, *59*, 1−36.
(25) Horsburgh, L. E.; Monkman, A. P.; Samuel, I. D. W. *Synth. Met.* **1999**, *101*, 113−114.
(26) Horsburgh, L. E.; Monkman, A. P.; Wang, C.; Bryce, M. R. *Mater. Res. Soc. Symp. Proc.* **2002**, *665*, 169−174.
(27) Sinha, S.; Rothe, C.; Beeby, A.; Horsburgh, L. E.; Monkman, A. P. *J. Chem. Phys.* **2002**, *117*, 2332−2336.
(28) Zhu, S. S.; Carroll, P. J.; Swager, T. M. *J. Am. Chem. Soc.* **1996**, *118*, 8713−8714.
(29) Delnoye, D. A. P.; Sijbesma, R. P.; Vekemans, J. A. J. M.; Meijer, E. W. *J. Am. Chem. Soc.* **1996**, *118*, 8717−8718.
(30) Ikkala, O.; Pietilä, L.-O.; Cao, Y.; Andretta, A. U.S. Patent 5,783,111, 1998.
(31) Monkman, A. P.; Halim, M.; Samuel, I. D. W.; Horsburgh, L. E. *J. Chem. Phys.* **1998**, *109*, 10372−10378.
(32) Monkman, A. P.; Pålsson, L.-O.; Higgins, R. W. T.; Wang, C.; Bryce, M. R.; Batsanov, A. S.; Howard, J. A. K. *J. Am. Chem. Soc.* **2002**, *124*, 6049−6055.
(33) Vanhee, S.; Rulkens, R.; Lehmann, U.; Rosenauer, C.; Schulze, M.; Köhler, W.; Wegner, G. *Macromolecules* **1996**, *29*, 5136−5142.
(34) Yun, H.; Kwei, T. K.; Okamoto, Y. *Macromolecules* **1997**, *30*, 4633−4638.
(35) Bjornholm, T.; Hassenkam, T.; Reitzel, N. *J. Mater. Chem.* **1999**, *9*, 1975−1990.
(36) Sirringhaus, H.; Brown, P. J.; Friend, R. H.; Nielsen, M. M.; Bechgaard, K.; Langeveld-Voss, B. M. W.; Spiering, A. J. H.; Janssen, R. A. J.; Meijer, E. W.; Herwig, P.; de Leeuw, D. M. *Nature* **1999**, *401*, 685−688.